Supporting Information for

Three Multi-responsive Luminescent Zn-CPs for Detection of Antibiotics/Cations/Anions in Aqueous Media

Chuanbin Fan,[a,b] Guimei Huang,[a,c] Zhiyong Xing,[a,b] Junli Wang,[a,b] Yaqin Pang,[a,b] Qingping Huang,[a,b] Shifu Huang,[a,b] Ziao Zong,[a,b,*] Feng Guo,[a,b,**]

a. School of Laboratory Medicine, Youjiang Medical University for Nationalities, Baise, Guangxi, 533000, P.R. China
b. Industrial College of Biomedicine and Health Industry, Youjiang Medical University for Nationalities, Baise, Guangxi, 533000, P.R. China
c. School of Chemistry and Pharmaceutical Sciences, Guangxi Normal University, Guilin 541004, People's Republic of China

*Corresponding author: zongziao@126.com.
**Corresponding author: guofeng1510@yeah.net.

Materials and General Characteristics

The used materials of this work were of AR grade and purchased from commercial sources without further purification. The experimental powder X-ray diffraction (PXRD) of **YMUN 6−8** samples were collected on a Rigaku Miniflex 600 instrument. A Nicolet 170SX spectrometer was employed to record the infrared (IR) spectra with KBr pellets, and the measurements were in the range of 4000−400 cm^{-1}. We used the Perkin-Elmer TG-7 thermogravimetric analyzer to conduct thermogravimetric analysis (TGA) under nitrogen condition, and the heating rate was 10 °C min^{-1} from 30 to 800 °C. A Shimadzu UV-2550 spectrophotometer was used to obtain the UV−vis spectra. Luminescence spectra were collected on a Perkin Elmer LS55 spectrophotometer.

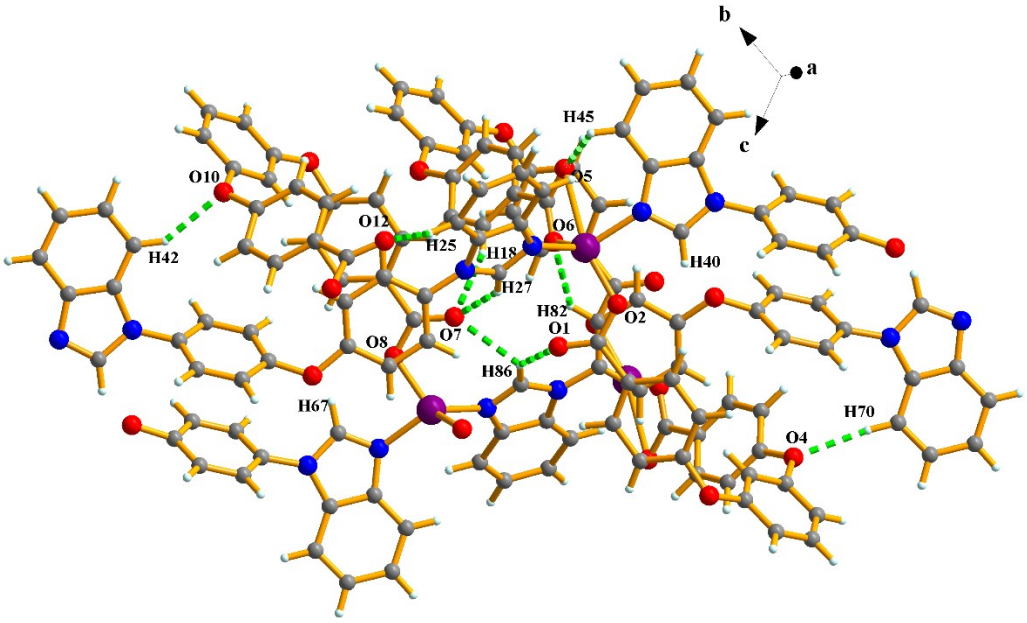

Figure S1. View of the noncovalent supramolecular interactions in YMUN **6**. The weak interactions in the neighboring A and B segments by C-H···O hydrogen bonding interactions (the distance of C-H···O and the angle of ∠C-H···O are listed in Table S2).

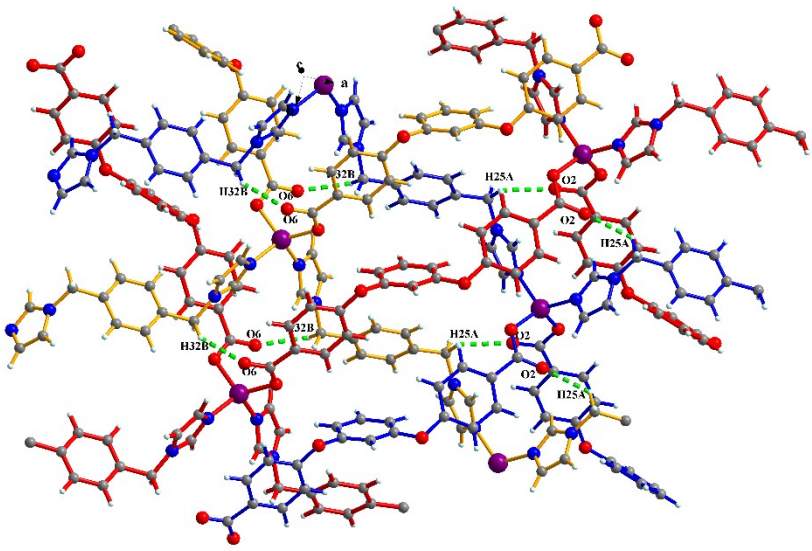

Figure S2. View of the noncovalent supramolecular interactions in YMUN **7**. The neighboring 2D three-fold interpenetrated structures are interlined by C-H···O hydrogen-bonding interactions (the distance of C-H···O and the angle of ∠C-H···O are listed in Table S2).

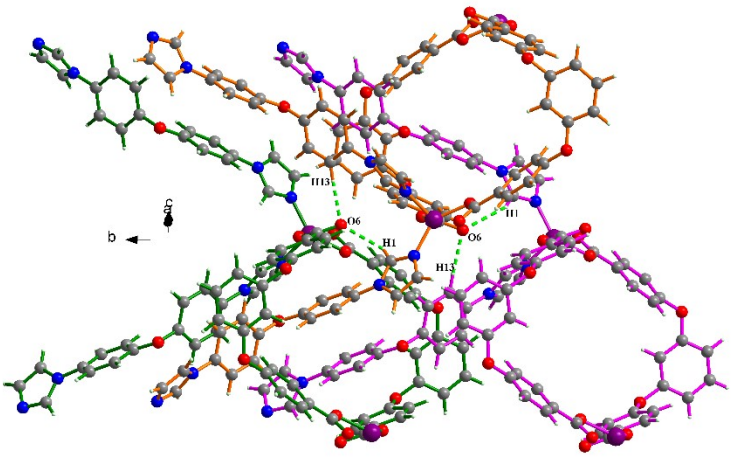

Figure S3. View of the noncovalent supramolecular interactions in YMUN **8**. The neighboring 2D three-fold interpenetrated structures are interlined by C-H···O hydrogen-bonding interactions (the distance of C-H···O and the angle of ∠C-H···O are listed in Table S2).

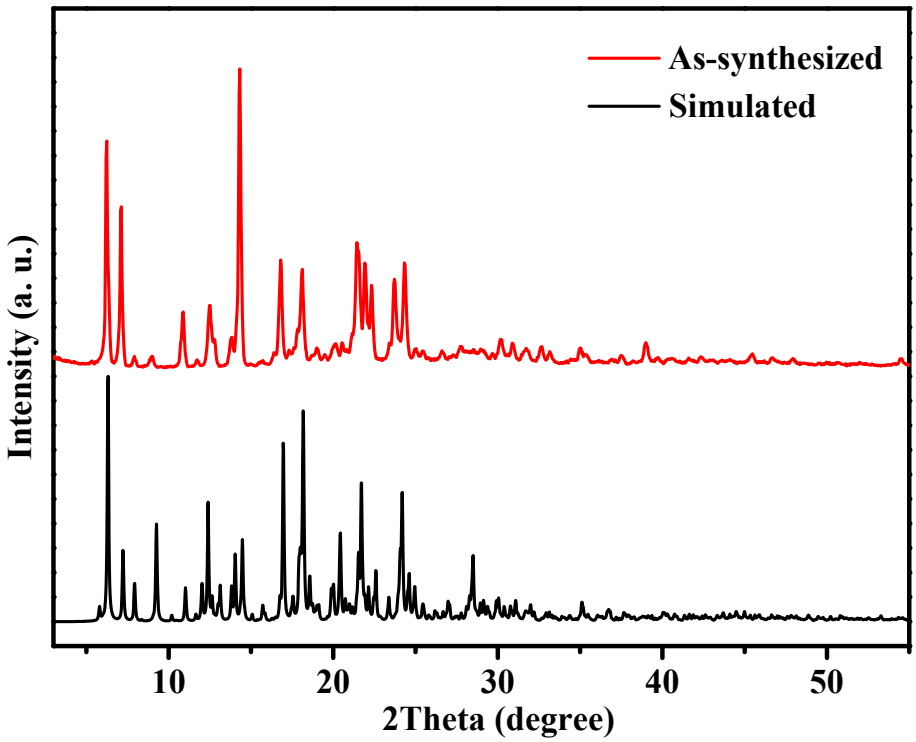

Figure S4. PXRD patterns of YMUN **6**, simulated and as-synthesized.

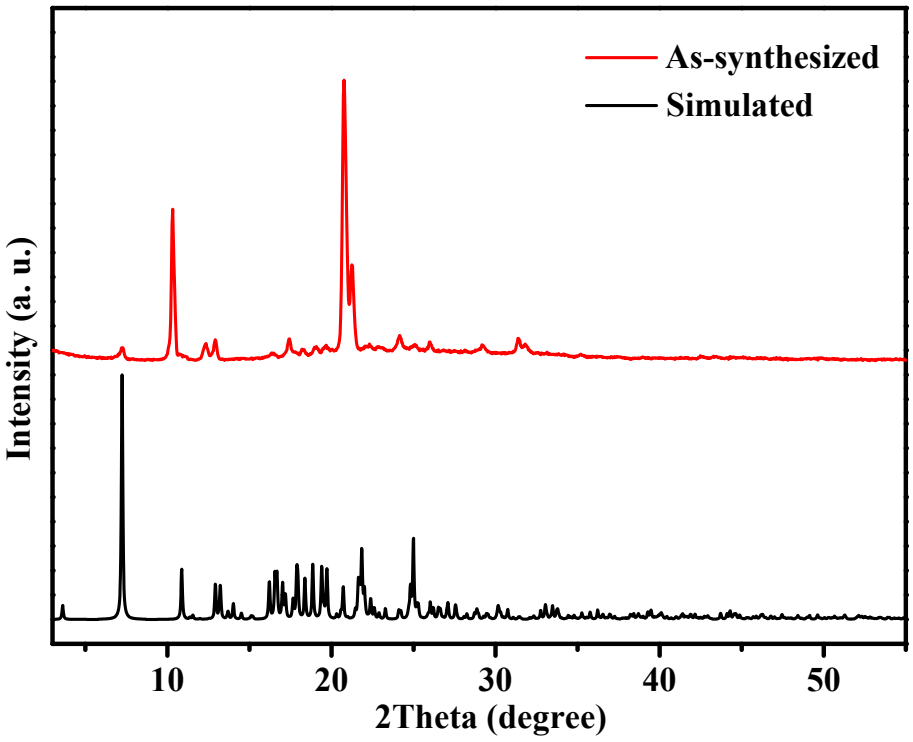

Figure S5. PXRD patterns of YMUN **7**, simulated and as-synthesized.

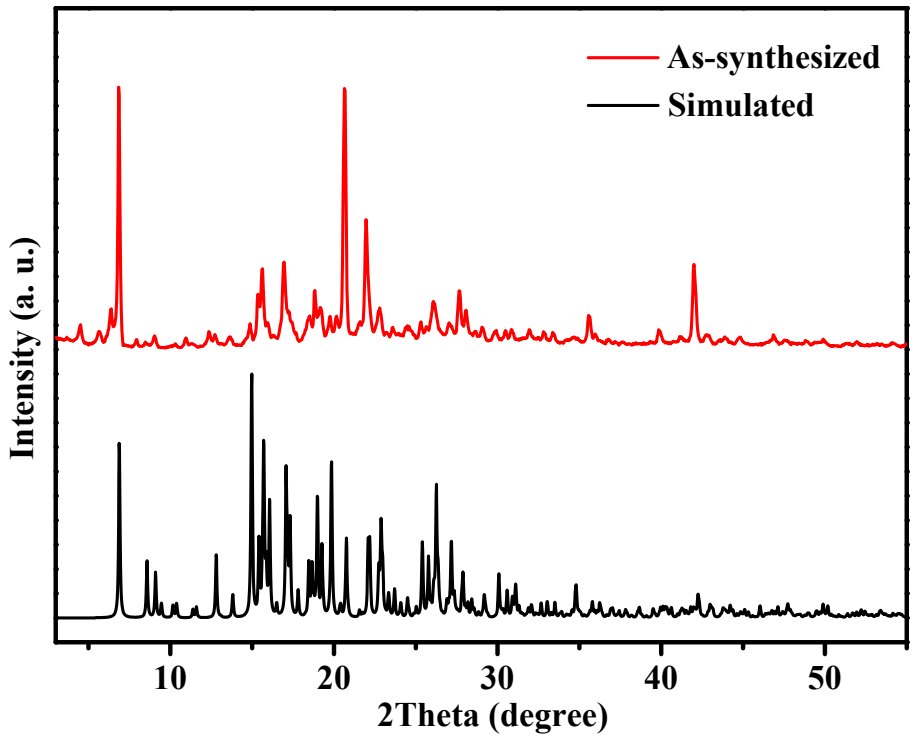

Figure S6. PXRD patterns of YMUN **8**, simulated and as-synthesized.

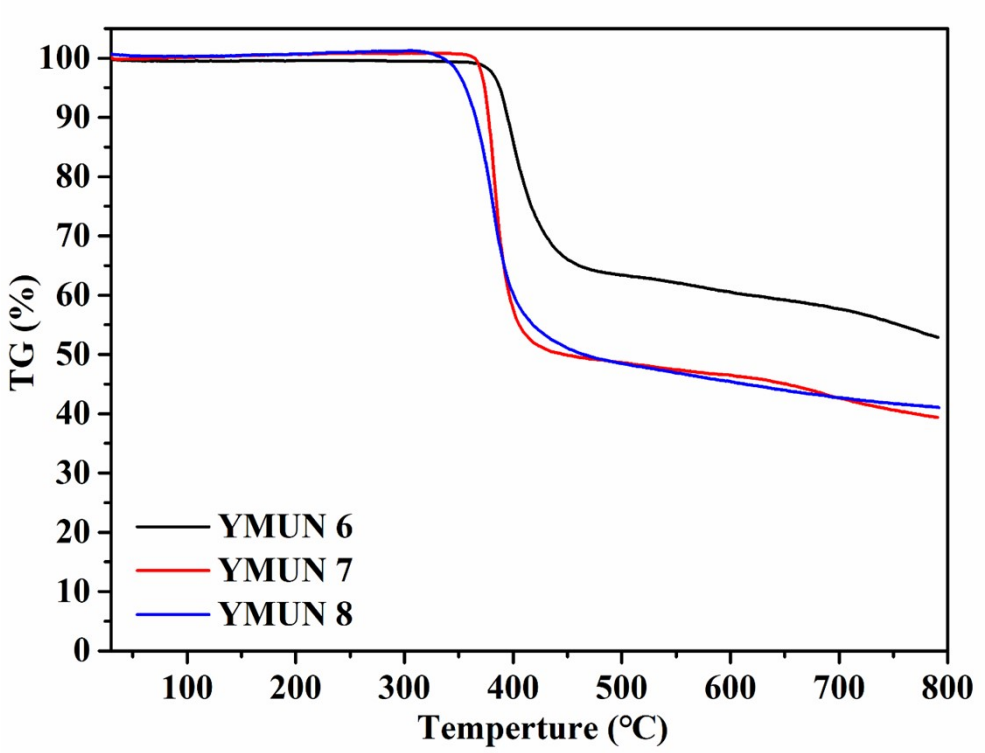

Figure S7. The TG curves of **YMUN 6–8**

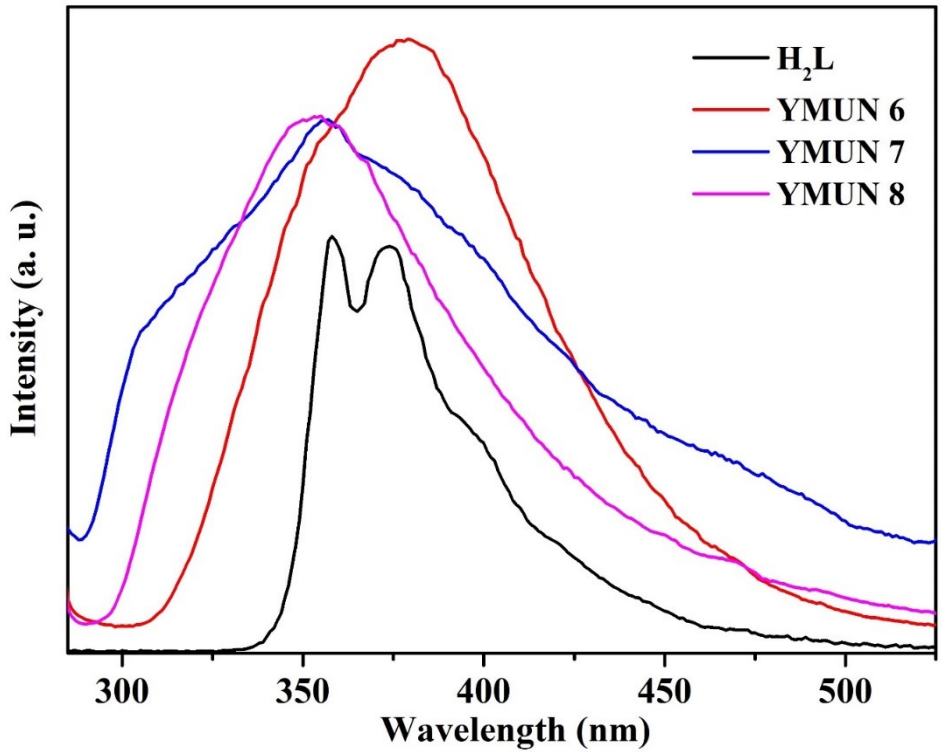

Figure S8. Photoluminescence of H_2L ligand and **YMUN 6–8** at room temperature in the solid state.

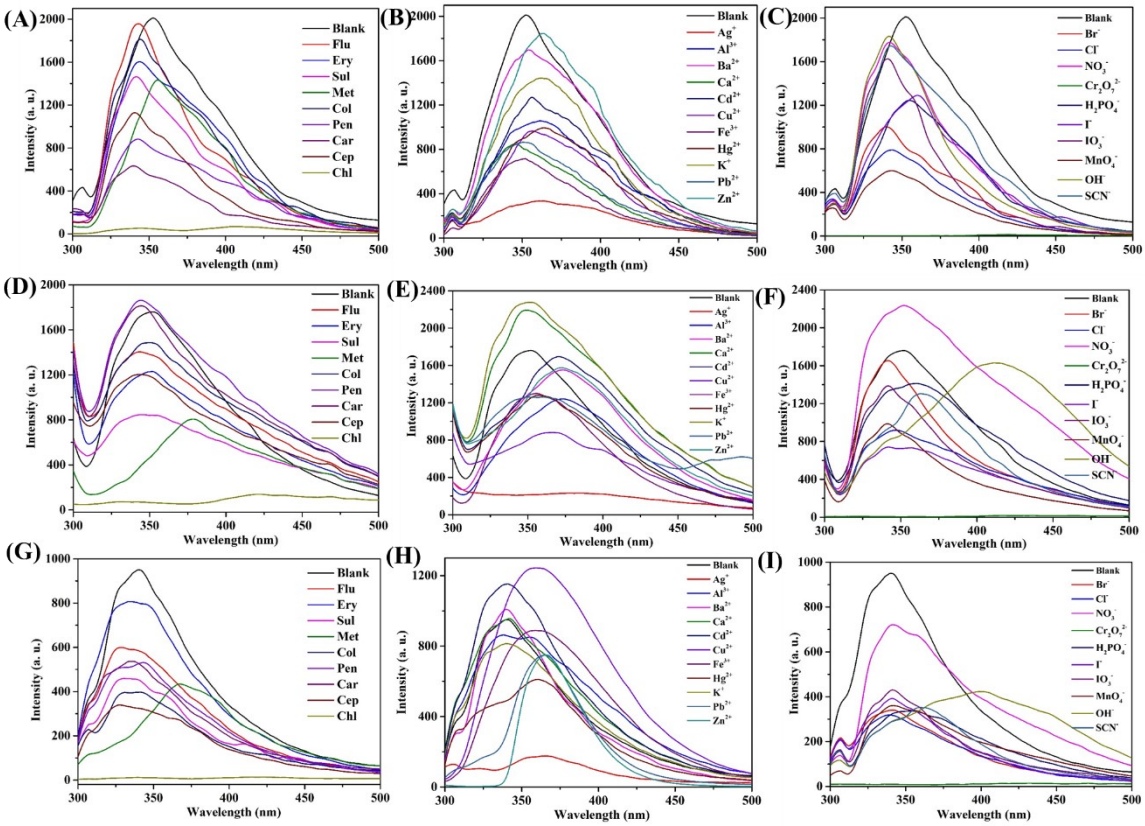

Figure S9. (A)-(C) Fluorescence spectra of **YMUN 6** powder and **YMUN 6** powder introduced into different antibiotics (0.5 mM), metal ions (1.0 mM), and cations (1.0 mM) in the aqueous solution at room temperature (λ_{ex} = 275 nm). (E)-(G) Fluorescence spectra of **YMUN 7** powder and **YMUN 7** powder introduced into different antibiotics (0.5 mM), metal ions (1.0 mM), and cations (1.0 mM) in the aqueous solution at room temperature (λ_{ex} = 271 nm). (G)-(I) Fluorescence spectra of **YMUN 8** powder and **YMUN 8** powder introduced into different antibiotics (0.5 mM), metal ions (1.0 mM), and cations (1.0 mM) in the aqueous solution at room temperature (λ_{ex} = 275 nm).

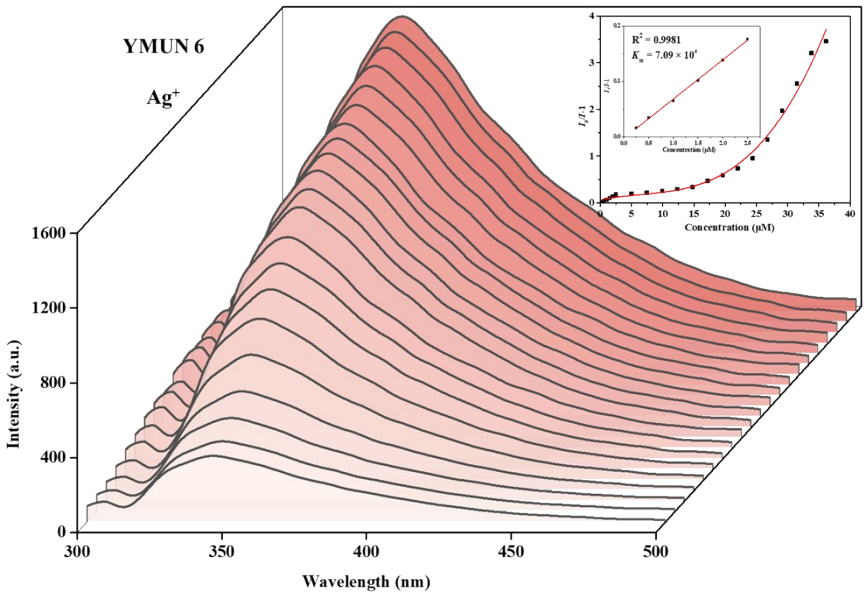

Figure S10. The fluorescence intensity trend spectra and the *S*−*V* linear relationship curve of **YMUN 6** after adding Ag^+ solution.

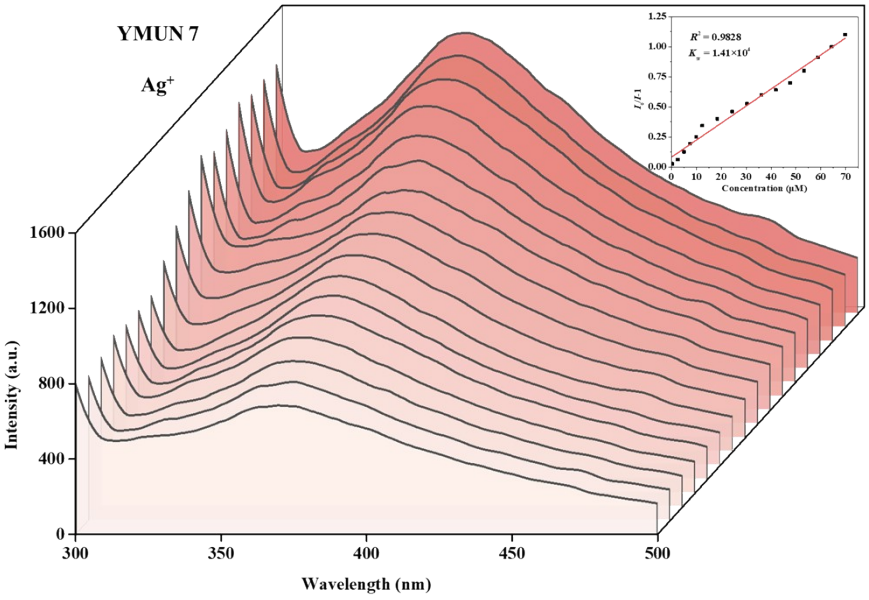

Figure S11. The fluorescence intensity trend spectra and the *S*−*V* linear relationship curve of **YMUN 7** after adding Ag^+ solution.

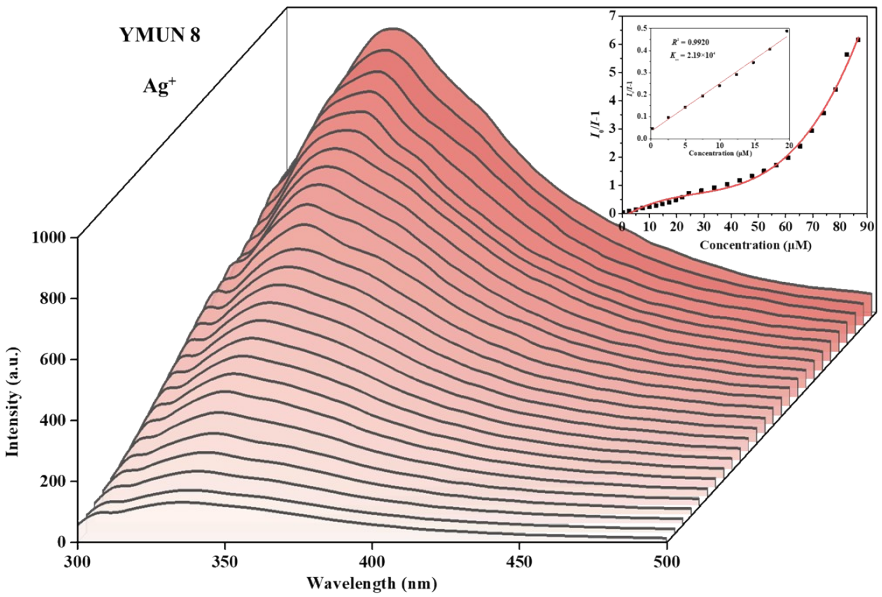

Figure S12. The fluorescence intensity trend spectra and the *S*−*V* linear relationship curve of **YMUN 8** after adding Ag^{+} solution.

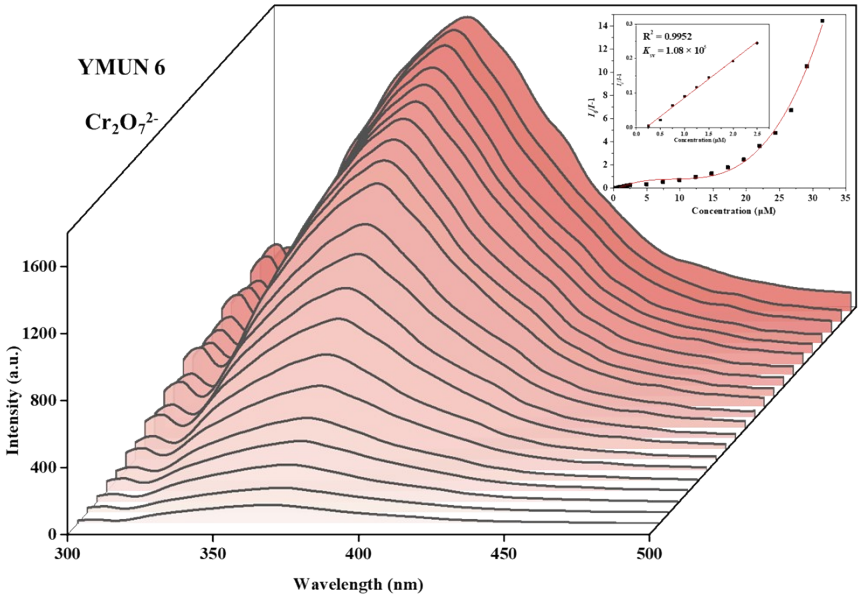

Figure S13. The fluorescence intensity trend spectra and the *S*−*V* linear relationship curve of **YMUN 6** after adding $Cr_2O_7^{2-}$ solution.

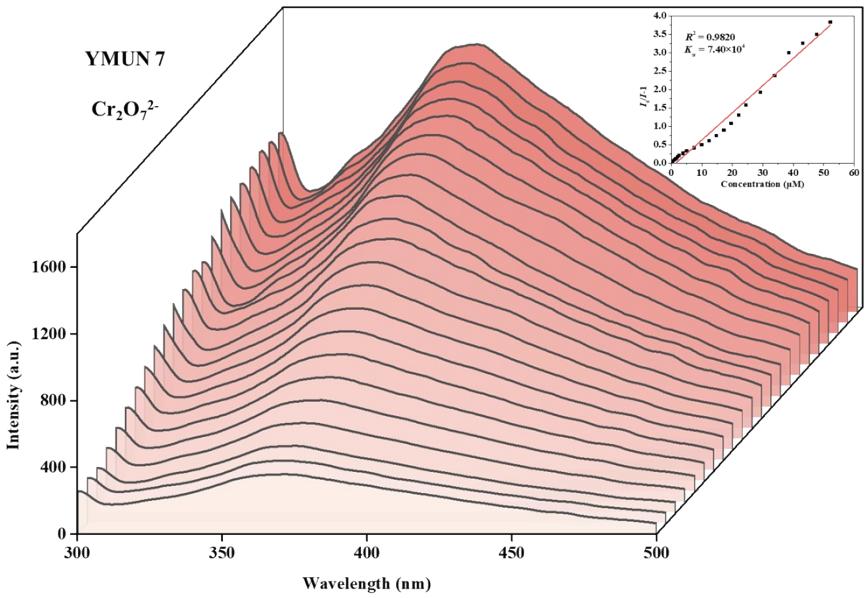

Figure S14. The fluorescence intensity trend spectra and the *S*−*V* linear relationship curve of **YMUN 7** after adding $Cr_2O_7^{2-}$ solution.

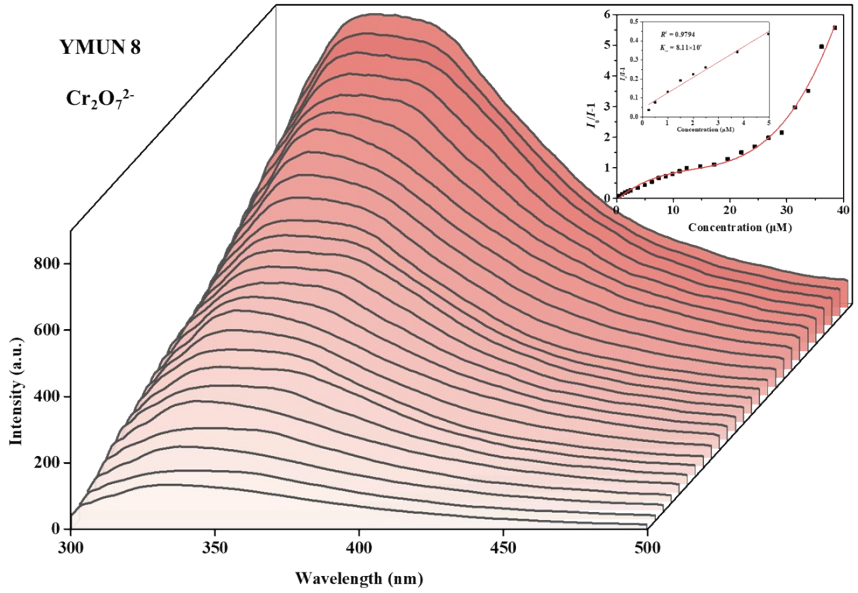

Figure S15. The fluorescence intensity trend spectra and the *S*−*V* linear relationship curve of **YMUN 8** after adding $Cr_2O_7^{2-}$ solution.

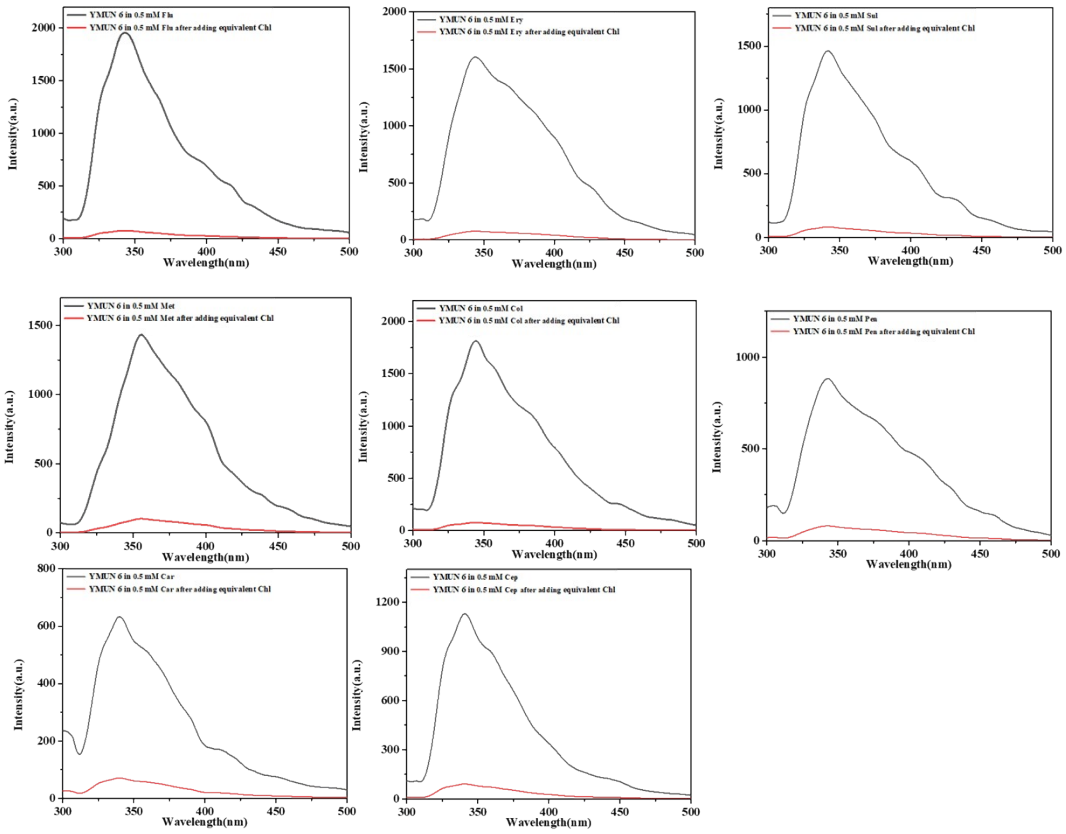

Figure S16. The fluorescence spectra of **YMUN 6** in various antibiotics (0.5 mM) (Black lines), and adding equivalent **Chl** in various antibiotics solution.

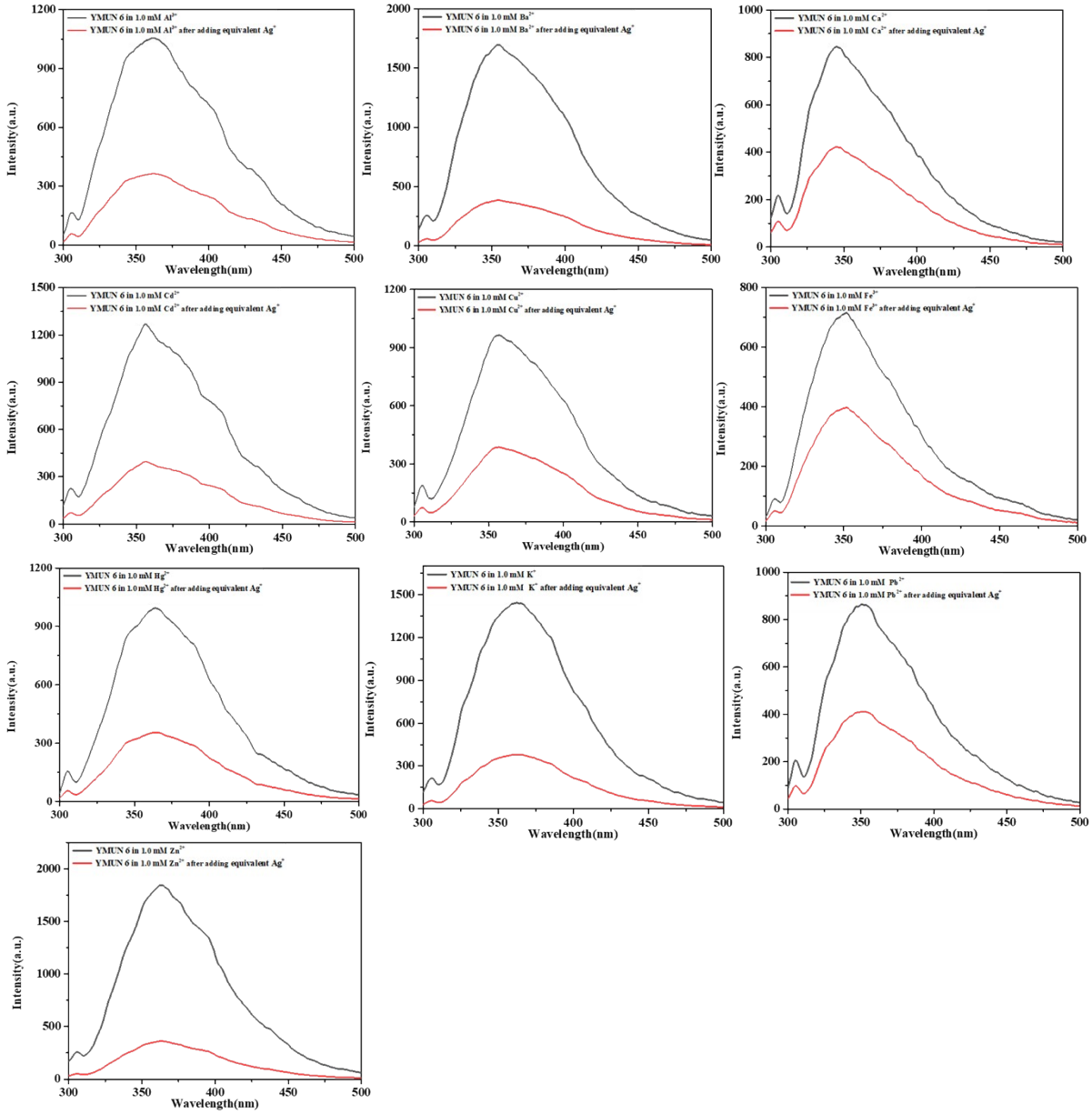

Figure S17. The fluorescence spectra of **YMUN 6** in various metal ions (1.0 mM) (Black lines), and adding equivalent Ag^{+} in various metal ions solution.

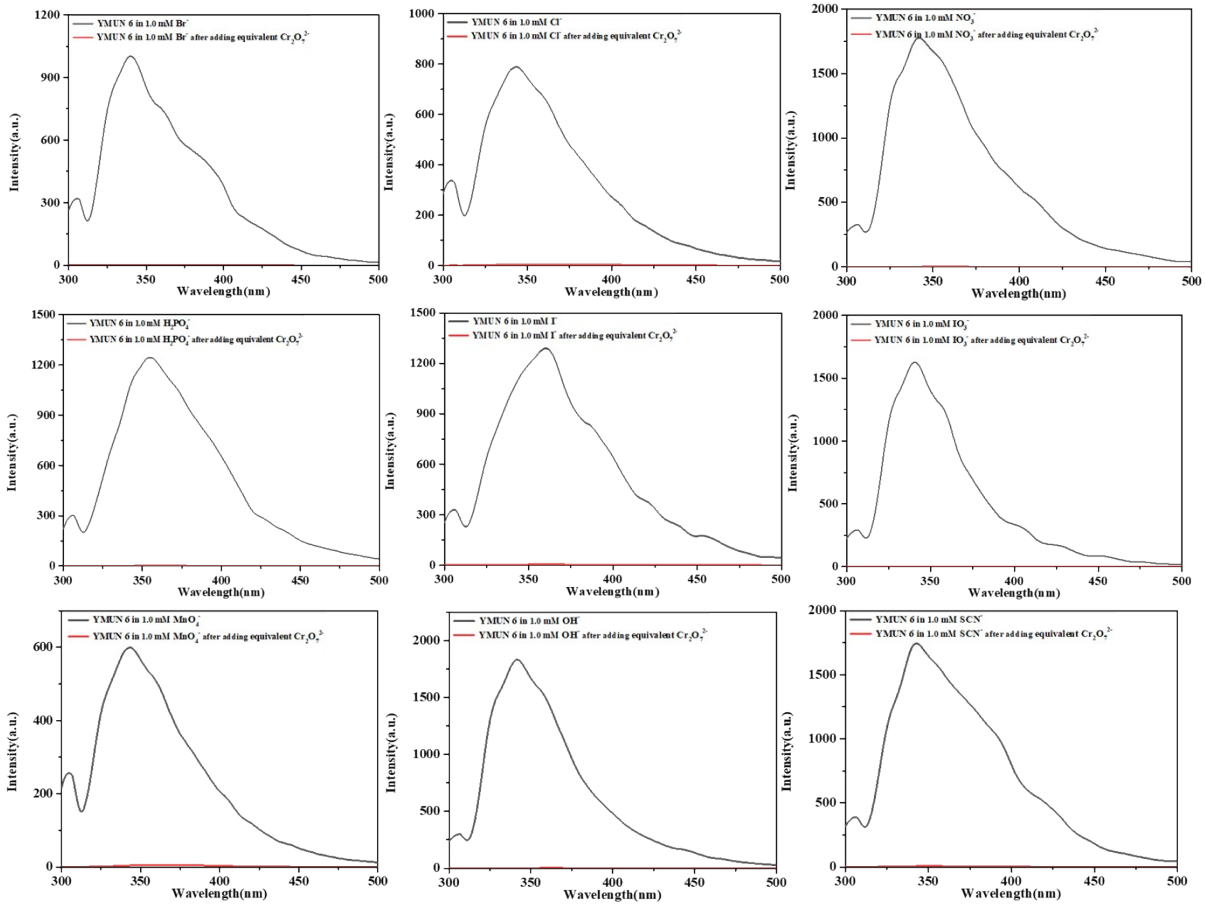

Figure S18. The fluorescence spectra of **YMUN 6** in various anions (1.0 mM) (Black lines), and adding equivalent $Cr_2O_7^{2-}$ in various anions solution.

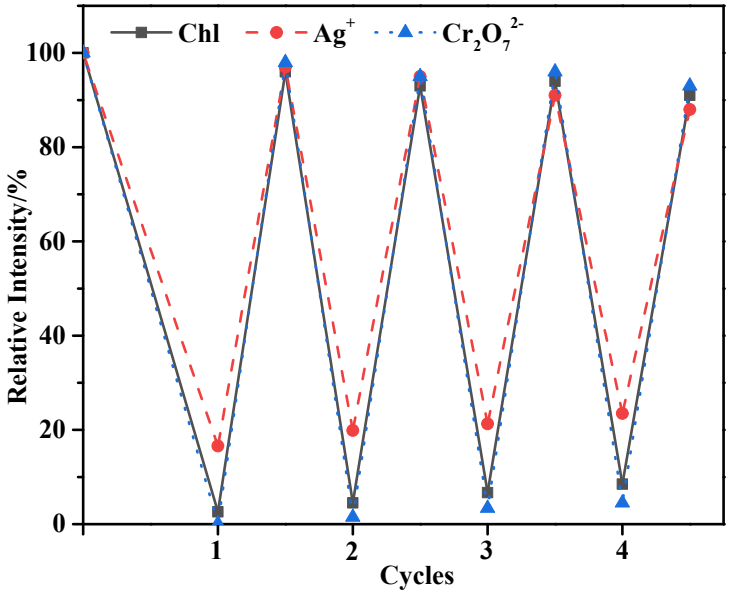

Figure S19. The recycling fluorescence intensity of **YMUN 6** for **Chl** antibiotic, Ag^+ ion, and $Cr_2O_7^{2-}$ ion, respectively, after four times.

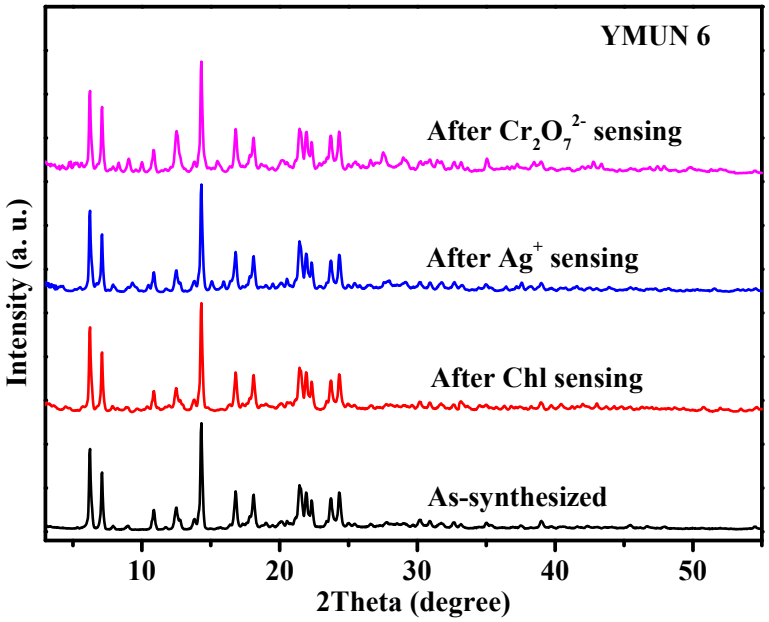

Figure S20. The comparison of PXRD patterns for **YMUN 6** after **Chl** antibiotic, Ag^+, $Cr_2O_7^{2-}$ ions sensing.

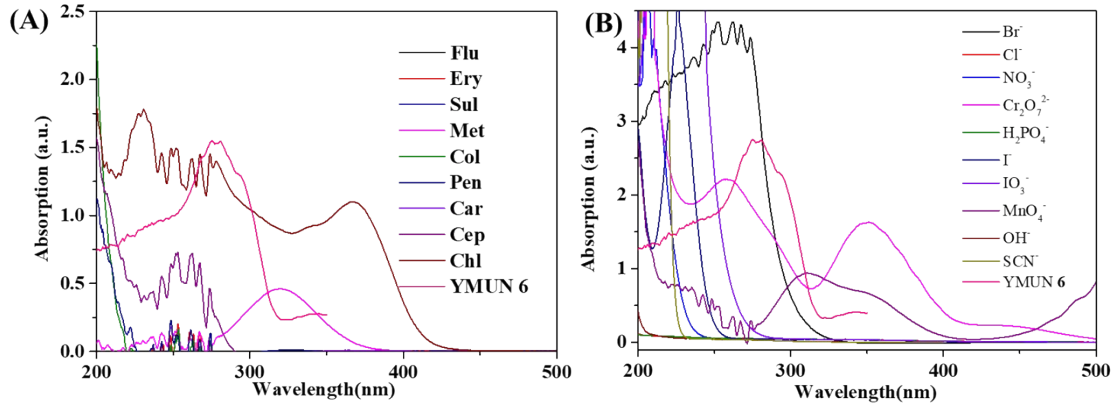

Figure S21. The UV-vis spectra of **Chl** antibiotic/$Cr_2O_7^{2-}$ ion in aqueous solutions and the excitation spectrum of **YMUN 6**.

Table S1 Selected bond lengths (Å) and angles (°) for **YMUN 6**–**8**.

YMUN 6			
Zn1—O2	1.968 (2)	Zn2—O8^{iii}	1.956 (2)
Zn1—O6^{i}	1.956 (2)	Zn2—O11	1.931 (2)
Zn1—N4^{ii}	2.022 (3)	Zn2—N8^{iv}	2.033 (3)
Zn1—N1	2.004 (3)	Zn2—N5	2.023 (3)
O2—Zn1—N4^{ii}	91.51 (11)	O6^{i}—Zn1—N1	98.39 (11)
O2—Zn1—N1	107.74 (11)	N1—Zn1—N4^{ii}	124.10 (12)
O6^{i}—Zn1—O2	117.63 (10)	O8^{iii}—Zn2—N8^{iv}	115.24 (11)

O6^{i}—Zn1—N4^{ii}	118.40 (11)	O8^{iii}—Zn2—N5	91.15 (11)
O11—Zn2—O8^{iii}	122.29 (11)	C1—O2—Zn1	120.1 (2)
O11—Zn2—N8^{iv}	95.87 (11)	C47—O8—Zn2^{iii}	115.4 (2)
O11—Zn2—N5	114.58 (11)	C66—O11—Zn2	122.4 (2)
N5—Zn2—N8^{iv}	119.90 (12)	C20—O6—Zn1^{i}	113.9 (2)
C87—N8—Zn2^{ii}	135.7 (2)	C46—N4—Zn1^{iv}	133.8 (2)
C86—N8—Zn2^{ii}	117.6 (2)	C40—N4—Zn1^{iv}	118.9 (2)
C21—N1—Zn1	137.2 (2)	C67—N5—Zn2	117.6 (2)
C27—N1—Zn1	116.9 (2)	C68—N5—Zn2	130.2 (2)

Symmetry codes: (i) -*x*, -*y*, -*z*; (ii) *x*, *y*-1, *z*-1; (iii) -*x*+1, -*y*+1, -*z*+1; (iv) *x*, *y*+1, *z*+1.

YMUN 7

Zn2—O5^{i}	1.977 (2)	Zn1—O1^{iv}	1.961 (2)
Zn2—O5	1.977 (2)	Zn1—O1	1.961 (2)
Zn2—N4^{ii}	2.026 (2)	Zn1—N1^{iv}	2.012 (3)
Zn2—N4^{iii}	2.026 (2)	Zn1—N1	2.012 (3)
O5^{i}—Zn2—O5	115.21 (14)	N4^{ii}—Zn2—N4^{iii}	108.02 (14)
O5^{i}—Zn2—N4^{iii}	118.02 (10)	O1^{iv}—Zn1—O1	119.21 (14)
O5^{i}—Zn2—N4^{ii}	99.20 (9)	O1^{iv}—Zn1—N1^{iv}	102.48 (10)
O5—Zn2—N4^{ii}	118.02 (10)	O1—Zn1—N1^{iv}	108.57 (10)
O5—Zn2—N4^{iii}	99.20 (9)	O1^{iv}—Zn1—N1	108.57 (10)
O1—Zn1—N1	102.48 (10)	N1^{iv}—Zn1—N1	116.23 (15)
N1^{iv}—Zn1—N1	116.23 (15)	C21—O5—Zn2	110.49 (19)
C21—O5—Zn2	110.49 (19)	C1—O1—Zn1	112.8 (2)
O1—Zn1—N1	102.48 (10)	C35—N4—Zn2^{v}	129.1 (2)
C24—N1—Zn1	132.5 (2)	C22—N1—Zn1	121.6 (2)

Symmetry codes: (i) -*x*+1, *y*, -*z*+3/2; (ii) -*x*+1, *y*-3, -*z*+3/2; (iii) *x*, *y*-3, *z*; (iv) -*x*+2, *y*, -*z*+3/2; (v) *x*, *y*+3, *z*.

YMUN 8

Zn1—O3	1.952 (2)	Zn1—N1	2.030 (3)
Zn1—O7^{i}	1.974 (2)	Zn1—N4^{ii}	2.048 (3)
O3—Zn1—O7^{i}	113.32 (11)	O7^{i}—Zn1—N1	95.75 (11)
O3—Zn1—N1	137.25 (12)	O7^{i}—Zn1—N4^{ii}	93.57 (11)

O3—Zn1—N4^{ii}	106.48 (11)	N1—Zn1—N4^{ii}	101.99 (12)
C19—O3—Zn1	104.9 (2)	C1—N1—Zn1	117.6 (3)
C38—O7—Zn1^{i}	120.6 (2)	C2—N1—Zn1	136.4 (2)
C18—N4—Zn1^{iii}	122.2 (2)	C17—N4—Zn1^{iii}	132.6 (3)

Symmetry codes: (i) -*x*+2, -*y*+2, -*z*+1; (ii) *x*+1/2, -*y*+1/2, *z*+1/2; (iii) *x*-1/2, -*y*+1/2, *z*-1/2.

Table S2 Hydrogen bond distances (Å) and angles (°) of **YMUN 6–8**

D-H···A	d(D-H)	d(H···A)	d(D···A)	∠DHA
YMUN 6				
C18-H18···O7	0.95	2.54	3.441(4)	159
C25-H25···O12	0.95	2.27	3.080(5)	143
C27-H27···O7	0.95	2.32	3.149(4)	145
C42-H42···O10	0.95	2.33	3.141(5)	143
C45-H45···O5	0.95	2.54	2.932(6)	105
C70-H70···O4	0.95	2.37	3.308(5)	171
C82-H82···O6	0.95	2.46	3.099(5)	124
C86-H86···O1	0.95	2.33	3.134(4)	142
C86-H86···O7	0.95	2.49	3.113(5)	123
YMUN 7				
C25-H25A···O2	0.99	2.47	3.061(4)	117
C32-H32B···O6	0.99	2.53	3.009(4)	109
YMUN 8				
C1-H1···O6	0.95	2.43	3.226(5)	141
C13-H13···O6	0.95	2.20	3.153(4)	178